Contents lists available at ScienceDirect

Applied Surface Science

Full Length Article

Ambient pressure X-ray photoelectron spectroscopy study of room-temperature oxygen adsorption on Cu(1 0 0) and Cu(1 1 1)

Bo-Hong Liu [a,*], Maximilian Huber [a,b,1], Matthijs A. van Spronsen [c,2], Miquel Salmeron [c], Hendrik Bluhm [a,d,3]

[a] Chemical Sciences Division, Lawrence Berkeley National Laboratory, Berkeley, CA 94720, USA
[b] Department of Chemistry, Technical University of Munich, D-85748 Garching, Germany
[c] Materials Sciences Division, Lawrence Berkeley National Laboratory, Berkeley, CA 94720, USA
[d] Advanced Light Source, Lawrence Berkeley National Laboratory, Berkeley, CA 94720, USA

ABSTRACT

We investigated the room-temperature chemisorption of oxygen on Cu(1 0 0) and Cu(1 1 1) using ambient-pressure X-ray photoelectron spectroscopy (APXPS). A shoulder-to-shoulder comparison between the oxygen-gas titration on the two surfaces reveals that Cu(1 0 0) is the more active for oxygen dissociative chemisorption when the surfaces are clean. The $(2\sqrt{2} \times \sqrt{2})$R45^o missing-row reconstruction appears in Cu(1 0 0)'s LEED image after about 10^4 Langmuir of oxygen exposure, whereas on Cu(1 1 1), no long-range ordering was observed throughout the whole experiment. An oxide layer consisting of cuprous and cupric oxide shows up on Cu(1 1 1) at an oxygen exposure that is significantly lower than for Cu(1 0 0). This observation suggests that the presence of $(2\sqrt{2} \times \sqrt{2})$R45^o missing-row reconstruction layer slows down Cu(1 0 0) oxidation. Literature has widely reported that surface morphology influences the copper oxidation process. This study provides an XPS demonstration that copper surface oxide formation in O_2 at room temperature depends on the surface crystallographic orientation.

1. Introduction

Upon exposure of copper to ambient or aerobic conditions, spontaneous surface oxidation occurs, resulting in changes in the surface properties. This native oxide layer influences the performance of copper-based applications, such as in semiconductor devices [1] and heterogeneous catalysis [2,3]. It also affects the corrosion behavior of copper-containing structures and devices. For example, a recent study showed that cupric (Cu(II)) oxide acts as an effective protective layer against further oxidation in electrochemical environments, while cuprous (Cu (I)) oxide is less protective [4]. The growth of a surface oxide layer on copper under ambient conditions proceeds on multiple temporal and length scales, resulting in a complex scenario [5]. In general, single-crystal studies agree that the native oxide layer growth starts with the formation of oxide nano-islands, which expand and coalesce into a fully extended layer that is epitaxial with the single-crystal substrate [5,6].

Further oxide growth beyond the initial stage is less understood at the atomic level.

Ultra-high vacuum-based surface-science techniques have long been used to study the interaction of low-index copper surfaces with oxygen gas [7–9]. At room temperature (RT), Cu(1 1 0), Cu(1 0 0), and Cu(1 1 1) all adsorb oxygen gas dissociatively. Cu(1 1 0) undergoes a (2x1) reconstruction with a half monolayer of oxygen coverage upon exposure to a few Langmuir (L) of O_2. The (2×1) structure evolves into a c(6 × 2) reconstruction, which contains two-third of surface oxygen coverage, after ∼ 100 L of oxygen exposure. For Cu(1 0 0), Simmons et al. showed that the "four-spot pattern" and c(2 × 2) (named Cu(1 0 0)p(1 × 1)-O in the original paper, corresponding to 0.5 ML of oxygen coverage) reconstructions appear when the surface is exposed to 1 L and 50 L of molecular oxygen, respectively [10]. The "four-spot pattern" was later studied in detail using a combination of low energy electron diffraction (LEED) and scanning tunneling microscopy (STM) by Fujita et al., who

* Corresponding author at: National Synchrotron Research Radiation Center, Hsinchu, Taiwan.
  E-mail address: Liu.bh@nsrrc.org.tw (B.-H. Liu).
[1] Current address: Department of Physics, Free University of Berlin, Berlin, Germany.
[2] Current address: Diamond Light Source Ltd., Didcot, Oxfordshire, United Kingdom.
[3] Current address: Department of Inorganic Chemistry, Fritz Haber Institute of the Max Planck Society, Berlin, Germany.

concluded that it originates from a c(4 × 6) superlattice with four orientations, with an overall surface oxygen coverage of 0.31 ML [11]. A (2√2 × √2)R45° missing-row (MR) reconstruction, with 0.5 ML of surface oxygen coverage, has frequently been reported for higher oxygen doses, although mild annealing is usually applied to enhance the ordering [12]. On Cu(111), no LEED pattern has been observed upon oxygen gas dosing at RT, even though STM investigations revealed substantial changes to the surface morphology at the local level [13–15]. Diffusion of atomic oxygen into the subsurface is more pronounced for Cu(111) than the other two surfaces, as concluded from the work function change upon oxygen dosing [16].

The abovementioned studies focused on the interaction of oxygen gas with copper single-crystal surfaces at oxygen pressures below 10^{-5} Torr. In the ambient condition, the copper oxide formed on copper metal surface has been studied using, e.g., X-ray absorption spectroscopy [17], X-ray diffraction [18], X-ray photoelectron spectroscopy [19], electron microscopy [20], and ellipsometry [21]. The three-step model for Cu oxide formation proposed by Platzman et al. is generally accepted [20]: (a) formation of a Cu_2O layer following a Cabrera-Mott model [22]; (b) the formation of a $Cu(OH)_2$ metastable overlayer, due to the interactions of Cu ions with hydroxyl groups present at the surface; and (c) the transformation of the $Cu(OH)_2$ metastable phase to a more stable CuO layer. However, not all studies agree with this model. For example, Chawla et al. concluded from X-ray photoelectron spectroscopy experiments that Cu_2O is the only oxide present after 24 h of exposure to air [19]. In another study, Lim et al. found that the texture and microstructure strongly influence the final structure of the oxide film [23]. On a uniform sample without apparent columnar structure and grain boundaries, they only observed the formation of cuprous oxide. However, "ambient" is not a well-defined condition. Factors like the relative humidity and the concentration of trace gases fluctuate geographically and temporally. Unfortunately, in investigations under ambient conditions, detailed environmental factors are rarely reported [5]. This might account for the diversity of results among those studies.

Over the past decades, a number of new developments in instrumentation have enabled surface science studies to be performed at pressures up to one atmosphere and beyond under well-controlled conditions [24], including studies of copper oxidation. For example, Zhou et al. investigated the oxidation kinetics of Cu(110), Cu(100), and Cu(111) with oxygen gas using transmission electron microscopy (TEM) [6]. Based on the change in morphology, the study showed that Cu(111) oxidation is dominated by the nucleation of oxide islands that coalesce into a Cu_2O layer at an oxygen pressure of $5 × 10^{-4}$ Torr and temperatures below 550 °C, whereas on both Cu(110) and Cu(100), oxidation is limited by oxygen diffusion. Although in this study, the chemical identity of the islands observed in the TEM images was not characterized, another TEM paper from Luo et al. concluded that the overlayer grown under similar conditions was comprised of Cu_2O, based on their electron diffraction experiment [25]. The same paper also reported that the interface of native Cu_2O with both Cu(111) and Cu(100) is epitaxial when the Cu_2O layer is formed under an oxygen pressure between $5 × 10^{-4}$ Torr and tens of Torr at 350 °C.

More information about the chemical identity of the oxygen-containing overlayer was reported in a study combining density functional theory and APXPS on the early-stage oxidation process on Cu (100) by Posada-Borbón et al. [26] They show that an oxygen adlayer forms when Cu(100) is exposed to 0.4 Torr of CO_2 at 100 °C. The oxygen layer evolved from a 0.25 monolayer (ML) p(2 × 2) structure to a 0.3 ML c(4 × 6) layer and finally formed a (2√2 × √2)R45° MR reconstruction layer, which contains 0.5 ML of surface oxygen. Parallel to that, an APXPS experiment by Wang et al. investigated the oxygen exposure on Cu(100) at 350 °C across a pressure range from 10^{-7} Torr to 1 Torr [27]. They concluded that the peak observed in the O 1 s spectrum in 10^{-7} Torr oxygen is due to the p(2 × 2) structure. This peak grew further between 10^{-6} and 10^{-3} Torr, which was ascribed to the formation of the (2√2 × √2)R45° MR reconstruction since the Cu 2p, and Cu LMM spectra did

not show any signs of oxide formation. Above 10^{-2} Torr, Cu_2O formation was observed, and finally, the topmost layers of the sample are further oxidized to CuO as the oxygen pressure increases to 1 Torr. The abovementioned two APXPS studies addressed the formation of oxygen adlayers and oxide layers on Cu(100) upon oxygen dosing. Unfortunately, other crystallographic orientations were not investigated, despite that Zhou et al. concluded that the surface oxide layer on different copper single crystal surfaces is formed via different kinetic pathways [6]. The aim of the present investigation is a comparative study of the room-temperature oxygen gas-induced oxidation of Cu (100) and Cu(111) under identical conditions using APXPS, with the goal to elucidating how the crystallographic orientation influences the oxygen uptake and the subsequent oxidation. No water or hydrogen is introduced into the chamber; therefore, we assume minimal hydroxyl species on the surface, if any, and do not include them in our discussion. Ex-situ LEED experiments were also performed for additional structural information.

1.1. Experimental

The experiments were performed at the APXPS-1 endstation [28] of beamline 11.0.2 [29] at the Advanced Light Source, Lawrence Berkeley National Laboratory. The base pressure of the XPS chamber was $2 × 10^{-9}$ Torr for both isotherm experiments reported in this paper. To regulate the oxygen pressures up to $1 × 10^{-4}$ Torr, the leak valve was pre-calibrated using an ion gauge so that the ion gauge could be turned off throughout the experiment. This prevents the experiment from being affected by a running ion gauge, as will be shown below. Pressures of $1 × 10^{-4}$ Torr and higher were monitored using a capacitance manometer (MKS, Baratron).

The Cu(111) and Cu(100) surfaces were cleaned in the preparation chamber (base pressure $5 × 10^{-10}$ Torr) by cycles of Argon sputtering (1 kV, $5 × 10^{-5}$ Torr) and annealing at 530 °C under UHV for 10 min until a sharp (1 × 1) pattern was observed by LEED and contaminations, including carbon and oxygen, became undetectable by XPS. The sample was heated using a ceramic-sealed boron-nitride heater (Heatwave Inc.). Beam-induced changes were monitored by measuring the O 1 s spectra at the end of every set of measurements at a fresh surface spot. No such changes were observed.

All XP spectra reported in this paper were taken with an electron analyzer pass energy of 20 eV. Cu $2p_{3/2}$ XP spectra were recorded at an incident photon energy of 1135 eV and O 1 s at 735 eV, i.e., both at a similar photoelectron kinetic energy of ~ 200 eV. Fitting the Cu $2p_{3/2}$ from the cleaned surfaces with Voigt function, the instrumental resolution is represented by the Gaussian width of 0.77 eV when the Lorentzian width be fixed at 0.56 eV [30]. All presented O 1 s spectra are normalized to the background region between 524 eV and 526 eV binding energy (BE), and Cu 2p spectra between 927.5 and 928.5 eV BE. The zero point of the BE scale was calibrated with the Fermi edge of metallic copper.

2. Results and discussion

The right panel of Fig. 1 shows the O 1 s XP spectra of Cu(100) exposed to increasing pressures and cumulative exposure of oxygen gas at room temperature. The O 1 s peak area w.r.t. the cumulative exposure before the oxide formation is summarized in Fig. 2. At $2 × 10^{-8}$ Torr, a peak emerges in the O 1 s spectrum slowly at 529.0 eV and continues to grow for up to 27 min at this pressure, corresponding to 32 L of O_2 exposure. The O 1 s grows further with oxygen pressure (10^{-7} Torr) and exposure (up to 118 L); under these conditions, its binding energy (BE) increases by 0.2 eV to 529.2 eV. A similar coverage-dependent O 1 s BE shift was reported previously by Tillborg et al. [31] and Posada-Borbón et al. [26], who attributed the shift to a change in oxygen adsorption site. As more oxygen is dosed, both the O 1 s peak area and position follow the same trend. At $5 × 10^4$ L/10^{-5} Torr of oxygen exposure, the
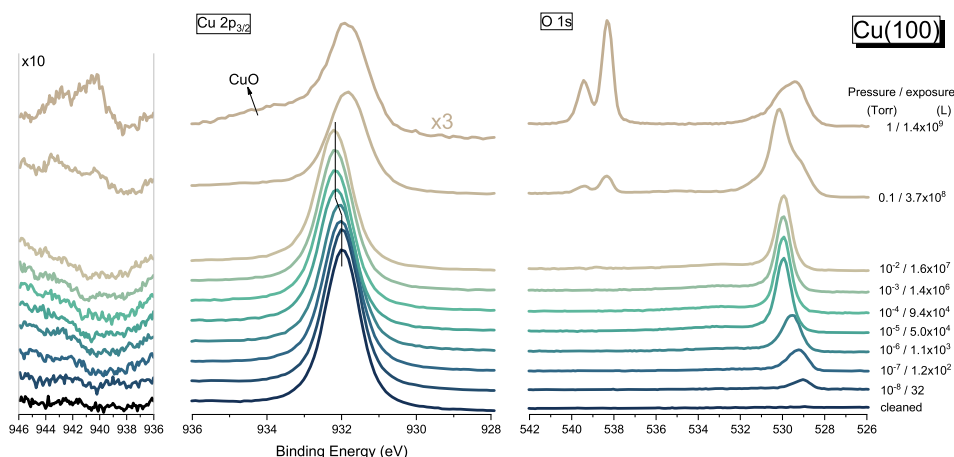
Fig. 1. Right panel: O 1s photoelectron spectra for Cu(100) exposed to oxygen gas at room temperature. The pressure (Torr) and the exposure (L) are indicated on the right. The doublet peaks around 539 eV are from gas phase oxygen. Middle panel: Cu $2p_{3/2}$ spectra for Cu(100) taken under the same condition as the O 1s spectra. The 1-Torr curve is tripled to reveal the indicated CuO feature. Left Panel: enlarged Cu(II) satellite region.
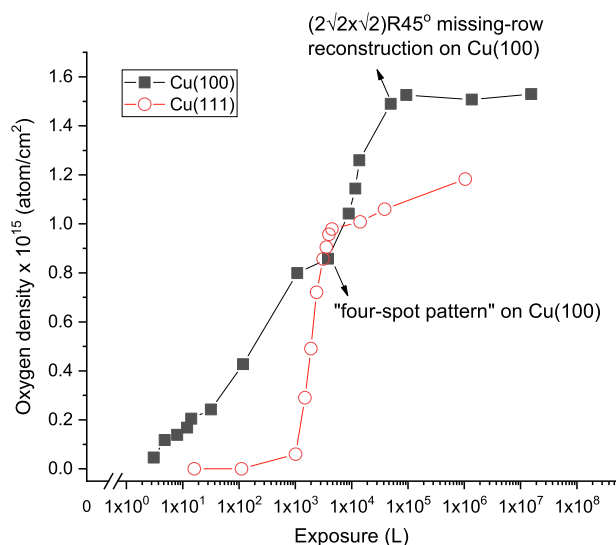

Fig. 2. Surface oxygen coverage on oxygen dosed Cu(100) and Cu(111) before the oxide layers appear. Based on the O 1 s peak areas, the coverage is normalized to the Cu(100)'s missing-row (MR) reconstruction layer, which has a half monolayer of oxygen coverage, corresponding to 1.53×10^{15} atom/cm². The data points are tabulated in table S2.

coverage by adsorbed oxygen saturates while the BE shifts by + 0.9 eV shift compared to the condition at the onset of oxygen adsorption. No further change to the O 1 s spectrum was observed up to an exposure of 1.6×10^7 L, reached in 10^{-2} Torr of oxygen gas pressure (see Fig. 2). Upon further exposure to oxygen, surface oxide formation is observed (see Fig. 1). The two peaks in the O 1 s spectra at 0.1 Torr are assigned to cuprous (530.1 eV) and cupric (529.2 eV) oxide, based on the reports by Platzman et al. [20], Stadnichenko et al. [32], and Jiang et al. [33]. The oxide layer growth saturated after 30 min in 0.1 Torr oxygen, as shown in fig. S1. Upon increasing the oxygen pressure to 1 Torr, the higher oxygen chemical potential from the gas phase drives the oxide layer composition towards cupric oxide, as shown in the corresponding O 1 s spectra.

The corresponding Cu $2p_{3/2}$ spectra from Cu(100), taken following the O 1 s spectra discussed above, are shown in the middle panel of Fig. 1. The BE of Cu $2p_{3/2}$ electrons documented in the literature for metallic copper, cuprous oxide, and cupric oxide are 932.6 eV, 932.4 eV, and 933.6 eV, respectively [33,34]. The absolute BE value alters from

instrument to instrument; however, the chemical shift is invariable. Since that the copper BE shift between metallic copper and cuprous oxide is only 0.2 eV, and that oxygen adsorption has minimal effect on the copper chemical shift, reliably fitting the Cu 2p spectra is not feasible at the spectrometer setting for copper 2p photoelectron measurement, where the instrumental resolution is 0.77 eV. As a compromise, the full-width at half-maximum (FWHM) of the Cu $2p_{3/2}$ peak envelope is used to probe the transition from metallic Cu to Cu(I). The FWHM of the Cu $2p_{3/2}$ peak as a function of oxygen exposure is shown in Fig. 3 and table S1. Referenced to the FWHM of metallic copper, the FWHM of Cu $2p_{3/2}$ broadens slightly by 0.02–0.03 eV after exposure to about 1000 L oxygen. Taking into account that the inelastic mean free path electrons with a kinetic energy of 200–eV in copper is ∼ 6 Å [35], and that the takeoff angle is around 42°, the XP signal in Fig. 1 represents mostly the top atomic layers. The topmost Cu layer partially covered by oxygen shows a BE shift, resulting in the broadening of the peak envelope. The peak broadening trend does not continue. As the oxygen exposure is increased up to 5×10^4 L, the Cu $2p_{3/2}$ peak's FWHMs narrows and returns to the value of the clean copper surface. The narrowing of FWHM can be associated with the completion of surface reconstruction resulting in formation of a uniform surface layer. We note that the Cu $2p_{3/2}$ BE also increases by 0.1–0.2 eV after the 5×10^4-L oxygen exposure, and the BE
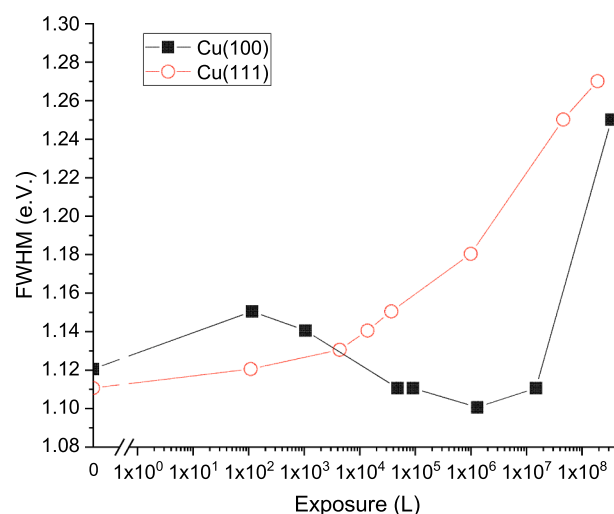

Fig. 3. Full-width at half-maximum of the Cu $2p_{3/2}$ peaks of Cu(100) and Cu (111) as a function of oxygen exposure. The fitting details are tabulated in table S1. Figure S4 shows representative fittings.

position of the valence band onset shifts by about the same amount, as shown in Fig. 4. This shift most likely reflects the opening of the band gap as the oxygen-bound copper dominates the surface, indicating a loss in metallicity. Consequently, the shift in Cu $2p_{3/2}$ cannot be assigned to a chemical shift, as the band bending in the depletion layer around the surface-bulk interface moves the BE of atoms in this layer [36]. Further oxygen exposure up to 1.6×10^7 L does not influent Cu $2p_{3/2}$, nor the O 1s spectrum. When the oxygen pressure is increased up to 0.1 Torr, the FWHM of Cu $2p_{3/2}$ increases significantly beyond 1.2 eV. This is most likely due to the mixed cuprous and cupric oxide layer on the surface, which agrees well with the assignment from the O 1 s spectra. The shake-up feature between 939 eV and 945 eV, shown in the left panel of Fig. 1, confirms the presence of Cu(II) even though it is barely detectable. The surface oxide layer grows as the O_2 pressure is further increased to 1 Torr, under which the Cu 2p spectra cannot be well-fitted with a single peak component anymore. A shoulder around 934 eV and the apparent shake-up feature indicate more Cu(II) on the surface.

We now turn our attention to the Cu(111) surface, where the effect of oxygen on the Cu surface chemistry differs from that observed on Cu (100). The RT isotherm of oxygen on Cu(111) is shown in Fig. 5. Below 10^{-7} Torr, no oxygen uptake is detectable within 5 min (i.e., below 300 L) in the O 1 s spectra. In 10^{-6} Torr oxygen, an O 1 s peak emerges and continues growing for 50 min, equivalent to 3000 L dosage. The onset for oxygen appearance on Cu(111) at 10^{-6} Torr oxygen pressure agrees with adsorption studies reported in the literature [14,37]. The O 1 s peak area increases by ∼ 20 % as the pressure is increased to 10^{-3} Torr and the exposure exceeds 10^6 L. In 10^{-2} Torr, the characteristic cuprous and cupric oxide peaks appear in the O 1 s spectrum at 530.1 eV and 529.2 eV, respectively. The ratio between the two peaks moves in favor of cupric oxide with increasing exposure from 1×10^6 to 4×10^7 L, as depicted in fig. S2. In addition, the overall area of the O 1 s peak envelope increases. This indicates a continuous oxygen uptake from the gas phase during this transformation. The composition of the surface oxide layer shifts towards cupric oxide as the oxygen pressure increases to 1 Torr.

The Cu $2p_{3/2}$ spectra acquired together with the Cu(111) O 1 s spectra are shown in the middle panel of Fig. 5. Again, the FWHM is used to indicate the change in the ratio of oxygen-bound copper to bare metallic copper, as depicted in Fig. 3 and summarized in table S1. The FWHM is 1.11 eV for both pristine Cu(111) and the Cu(111) in 1×10^{-7} Torr oxygen. The FWHM increases to 1.13 eV as the oxygen pressure increases to 1×10^{-6} Torr and continues to broaden to 1.18 eV as the oxygen pressure rises to 1×10^{-3} Torr. Most likely, the broadening is due
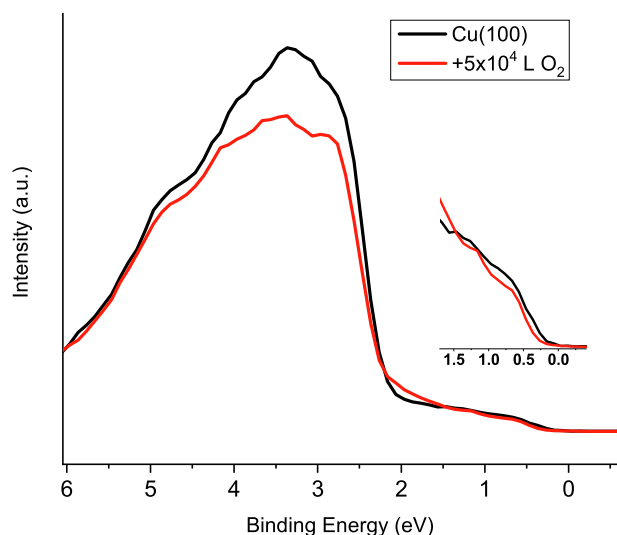
to the appearance of chemisorbed oxygen. At 1×10^{-2} Torr oxygen, the Cu $2p_{3/2}$ peak FWHM increases considerably, most likely due to the formation of an oxide layer. The broadening of the Cu $2p_{3/2}$ peak continues as the oxygen pressure is increased to 0.1 Torr and finally to 1 Torr. The shake-up features between 938 and 945 eV become prominent at 1 Torr oxygen, indicating a significant enhancement of cupric oxide at the surface.

To gain further structural information, we perform an ex-situ low energy electron diffraction (LEED) investigation on Cu(100) and Cu (111) after room temperature oxygen exposures. To that end, after certain exposure times to oxygen, the sample was transferred to the preparation chamber and there investigated in vacuum. In the case of Cu (111), no diffraction pattern was observed on Cu(111) in all cases. Cu (100), however, showed clear LEED patterns in the form of two superstructures. The first structure appears after placing the Cu(100) in 10^{-5} Torr oxygen gas for 10 s, after which the cumulative dose reached 3800 L. As shown in fig. S3(b), a weak "four-spot pattern" emerged on Cu (100). This faint pattern was first reported by Simmons et al. [10] Using STM [11], Fujita et al. concluded that this pattern originates from nanometer-sized antiphase c(2×2) domains. Although this antiphase c (2×2) structure possesses no long-range order, a new emerging periodicity that consists of local c(2×2) domains and the zigzag-shaped domain boundaries generate the four-spot LEED pattern. Another structure that produces a $(2\sqrt{2} \times \sqrt{2})R45^o$ LEED pattern, shown in fig. S3(c), appears after exposure at 10^{-5} Torr for an hour, which corresponds to 5×10^4 L. This structure is referred to as the missing-row (MR) reconstruction in the literature. Usually, this MR reconstruction is grown by exposing Cu(100) to oxygen gas at elevated temperatures instead of the RT in this study.[12,38] According to the atomic model reported, the oxygen coverage of this MR reconstruction surface layer is 0.50 ML, which translates to 1.53×10^{15} atom/cm^2. We use this value to normalize the O 1 s signal at various stages of exposures into coverage values, as summarized in table S2.

The experiments shown above demonstrate that the two copper single crystal facets react differently to room-temperature oxygen exposure. Whereas Cu(100) has a lower onset pressure for oxygen chemisorption, Cu(111) obtains a full oxide layer at a lower oxygen pressure and exposure. The former observation agrees with previous studies, which concluded that Cu(100) is more reactive than Cu(111) towards oxygen dissociation at RT, owing to its more open surface [5,39,40]. The latter observation, however, suggests a difference in the mechanism that governs the formation of native oxide layers on the two surfaces. From a thermodynamic viewpoint, one might speculate that the formation of the epitaxial interface, whose stability is correlated to the degree of lattice matching, may account for the tendency for surface oxide layer formation. This is based on Ketteler et al.'s report that a metastable subsurface oxide layer on Pd(111) is more easily observed than a bulk oxide layer, as the former has a better lattice matching to Pd (111), resulting in a more stable interface [41]. However, the interface epitaxy in the present case does not seem to account for the different native oxide-forming mechanisms on Cu(100) and Cu(111). As Luo et al.'s study shows, both Cu(111) and Cu(100) have an epitaxial interface with the native Cu_2O layer, which grew upon exposing the surface to oxygen in the Torr-range pressures at 350 °C [25]. Their electron diffraction experiments revealed that the epitaxy on Cu(111) is $(111)Cu_2O||(111)Cu$ and $[110]Cu_2O||[110]Cu$, whereas on Cu(100) it is $(100)Cu_2O||(100)Cu$ and $[110]Cu_2O||[110]Cu$. The lattice mismatch in both cases is 18%; therefore, it cannot explain the different native oxide-forming behavior on Cu(111) and Cu(100). A more plausible scheme is that those two surfaces generate the native oxide layer via different pathways. As Lee et al. pointed out in their DFT study for Cu(100) oxidation, a Cu_2O oxide-like layer structure, arguably the precursor of the Cu_2O layer, grows on the surface via transformation of the $(2\sqrt{2} \times \sqrt{2})R45^o$ MR structure [42]. From a thermodynamic point of view, the extra potential needed to drive the transformation depends
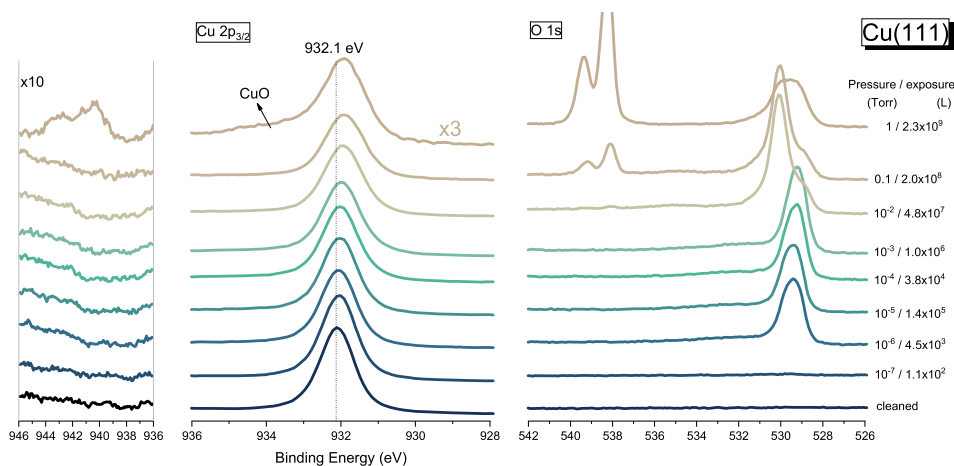

Fig. 4. Valence band spectra of clean Cu(100) and after dosing 5×10^4 L of oxygen.

Fig. 5. Right panel: O 1s photoelectron spectra for Cu(1 1 1) exposed to oxygen gas at room temperature. The pressure (Torr) and the exposure (L) are indicated on the right. The doublet peaks around 539 eV are from gas phase oxygen. Middle panel: Cu $2p_{3/2}$ spectra for Cu(1 1 1) taken under the same condition as the O 1s spectra. The 1-Torr curve is tripled to reveal the indicated CuO feature. Left Panel: enlarged Cu(II) satellite region.

on the stability of the $(2\sqrt{2} \times \sqrt{2})R45^o$ MR structure, which is arguably fairly stable, as it has been frequently observed and reported in the literature [26,43,44]. Lee et al. also pointed out that subsurface oxygen is crucial for transforming the $(2\sqrt{2} \times \sqrt{2})R45^o$ MR structure to an oxide layer, whereas the surface oxygen plays a minor role. On the basis of these considerations, one might speculate that from a kinetic stand-point, the $(2\sqrt{2} \times \sqrt{2})R45^o$ MR layer may alter the abundance of sub-surface oxygen, as its oxygen dissociation activity and oxygen permeability are different from the pristine Cu(1 0 0). Unfortunately, we could not see any sign of subsurface oxygen in the XPS spectra. The probing-depth limit imposed by the beamline's photon energy restricts us from verifying this hypothesis. The oxide layer formation rate may be altered as a consequence. These may explain the phenomenological passivating behavior of the $(2\sqrt{2} \times \sqrt{2})R45^o$ MR layer. These schemes are valid only for Cu(1 0 0) oxidation, as no such reconstruction has been observed so far on Cu(1 1 1).

In a final remark, we note that it was important to take care to prevent the interference of an operating (hot filament) ion gauge on the oxidation chemistry during our experiment. By pre-calibrating the leak valve, the ion gauge could remain turned off throughout oxygen expo-sure in our experiments. Interference of an operating ion gauge on APXPS experiments was reported previously by Trotochaud et al., who showed a partial reduction of Cu(II) to Cu(I) on a CuO foil sample when the ion gauge was turned on under 10^{-4} Torr of water vapor pressure; also, the same condition enhances hydroxylation on both CuO and Cu₂O foils [45]. During our experiments, we observed the influence of the ion gauge on the spectra of both Cu(1 1 1) and Cu(1 0 0) at the oxygen pressure of 10^{-4} Torr. Fig. 6 shows data from an experiment on a Cu (1 1 1) which had gone through the whole set of oxygen exposure as shown in Fig. 1, now placed in 10^{-4} Torr of oxygen while ion gauge turned on. The 933.2 eV peak in Fig. 6 and the shake-up feature of CuO grew at the expense of the 931.9 eV peak. This indicates further oxidation of the surface/subsurface Cu(I) to Cu(II). This phenomenon is neither seen when the ion gauge is turned off nor when the pressure is below 10^{-4} Torr. We note that averting the sample surface from the line of sight of the ion gauge filament does not reduce the effect. It seems that the ion gauge operating in 10^{-4} Torr oxygen has a significant discharge current and acts as an efficient source for reactive oxygen species, such as ozone and atomic oxygen. These reactive oxygen species then migrate to the sample and oxidize the surface, after several collisions with parts of the interior of the chamber, whose principle dimension is much longer than the inelastic mean free path of several tens of cm at this oxygen gas pressure. Based on our observation, along with that from Trotochaud et al., we suggest that the influence of an operating ion gauge on the
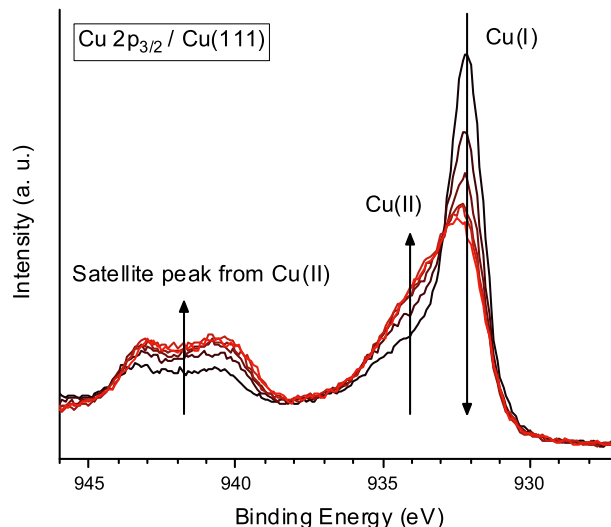

Fig. 6. A series of Cu $2p_{3/2}$ spectra showing the effect of 10^{-4} Torr oxygen gas while a hot-filament ion gauge was turned on all the time. The time interval between each spectrum is 7.5 min. The time lapse between the first and the last spectrum is 37 min. Notice that the starting point of this experiment is the Cu (1 1 1) sample after the isotherm experiment that forms a surface oxide layer. The same effect was seen on Cu(1 0 0) as well.

surface chemistry has to be carefully controlled, particularly at or close to 10^{-4} Torr. A cold cathode gauge could be more suitable for APXPS setups.

3. Conclusion

Room-temperature oxygen gas exposure to Cu(1 1 1) and Cu(1 0 0) has been studied using APXPS and LEED. At low pressure, dissociative adsorption of oxygen occurs more easily on Cu(1 0 0) than Cu(1 1 1). At higher oxygen pressures and exposures, a copper oxide layer appears on Cu(1 1 1) at a pressure and exposure lower than for Cu(1 0 0). The presence of $(2\sqrt{2} \times \sqrt{2})R45^o$ missing-row reconstruction layer on Cu (1 0 0) seems to slow down its oxidation, an observation that can be rationalized from both thermodynamic and kinetic viewpoints. The hot filament of the operating ion gauge induces the formation of reactive oxygen species which facilitate oxidation of the sample at already 10^{-4} Torr oxygen, a factor that needs to be taken into account in studies of the oxidation of metals and semiconductors under intermediate oxygen

pressures.

CRediT authorship contribution statement

Bo-Hong Liu: Conceptualization, Methodology, Formal analysis, Investigation, Data curation, Writing – original draft, Visualization. **Maximilian Huber:** Investigation. **Matthijs A. van Spronsen:** Investigation, Writing – review & editing. **Miquel Salmeron:** Validation, Resources, Writing – review & editing, Funding acquisition. **Hendrik Bluhm:** Validation, Resources, Writing – review & editing, Supervision, Funding acquisition.

Declaration of Competing Interest

The authors declare that they have no known competing financial interests or personal relationships that could have appeared to influence the work reported in this paper.

Acknowledgements

Appendix A. Supplementary material

Supplementary data to this article can be found online at https://doi.org/10.1016/j.apsusc.2022.152438.

References

[1] B.K. Meyer, A. Polity, D. Reppin, M. Becker, P. Hering, P.J. Klar, T.h. Sander, C. Reindl, J. Benz, M. Eickhoff, C. Heiliger, M. Heinemann, J. Bläsing, A. Krost, S. Shokovets, C. Müller, C. Ronning, Binary copper oxide semiconductors: From materials towards devices, Physica Status Solidi B-Basic Solid State Physics 249 (8) (2012) 1487–1509.

[2] M. Behrens, Heterogeneous Catalysis of CO2 Conversion to Methanol on Copper Surfaces, Angewandte Chemie-International Edition 53 (45) (2014) 12022–12024.

[3] G.G. Jernigan, G.A. Somorjai, Carbon-monoxide oxidation over 3 different oxidation-states of copper - metallic copper, copper (I) oxide, and copper (II) oxide - a surface science and kinetic-study, J. Catal. 147 (2) (1994) 567–577.

[4] E. Touzé, C. Cougnon, Study of the air-formed oxide layer at the copper surface and its impact on the copper corrosion in an aggressive chloride medium, Electrochim. Acta 262 (2018) 206–213.

[5] C. Gattinoni, A. Michaelides, Atomistic details of oxide surfaces and surface oxidation: the example of copper and its oxides, Surf. Sci. Rep. 70 (3) (2015) 424–447.

[6] G. Zhou, J.C. Yang, Initial oxidation kinetics of Cu(100), (110), and (111) thin films investigated by in situ ultra-high-vacuum transmission electron microscopy, J. Mater. Res. 20 (7) (2005) 1684–1694.

[7] G. Ertl, Untersuchung Von Oberflachenreaktionen Mittels Beugung Langsamer Elktronen (LEED). I. Wechselwirkung Von O2 und N2O MIT (110)-(111)-und (100)-Kupfer-Oberflachen, Surf. Sci. 6 (2) (1967) 208–1000.

[8] T.A. Delchar, Oxygen chemisorption on copper single crystals, Surf. Sci. 27 (1) (1971) 11–20.

[9] F. Besenbacher, J.K. Nørskov, Oxygen-chemisorption on metal-surfaces - general trends for CU, NI and AG, Prog. Surf. Sci. 44 (1) (1993) 5–66.

[10] G.W. Simmons, D.F. Mitchell, K.R. Lawless, Leed and heed studies of interaction of oxygen with single crystal surfaces of copper, Surf. Sci. 8 (1–2) (1967) 130–1000.

[11] T. Fujita, Y. Okawa, Y. Matsumoto, K. Tanaka, Phase boundaries of nanometer scale c(2x2)-O domains on the Cu(100) surface, Phys. Rev. B 54 (3) (1996) 2167–2174.

[12] J.H. Onuferko, D.P. Woodruff, Leed structural study of the adsorption of oxygen on CU(100) surfaces, Surf. Sci. 95 (2-3) (1980) 555–570.

[13] F. Wiame, V. Maurice, P. Marcus, Initial stages of oxidation of Cu(111), Surf. Sci. 601 (5) (2007) 1193–1204.

[14] H.M. Altass, HCl Nanoscience at Copper and Copper/Gold Alloy Surfaces. Cardiff University, 2013.

[15] B. Eren, L. Lichtenstein, C.H. Wu, H. Bluhm, G.A. Somorjai, M. Salmeron, Reaction of CO with Preadsorbed Oxygen on Low-Index Copper Surfaces: An Ambient Pressure X-ray Photoelectron Spectroscopy and Scanning Tunneling Microscopy Study, J. Phys. Chem. C 119 (26) (2015) 14669–14674.

[16] A. Spitzer, H. Lüth, The adsorption of oxygen on copper surfaces.2. CU(111), Surf. Sci. 118 (1-2) (1982) 136–144.

[17] P. Keil, R. Frahm, D. Lützenkirchen-Hecht, Native oxidation of sputter deposited polycrystalline copper thin films during short and long exposure times: Comparative investigation by specular and non-specular grazing incidence X-ray absorption spectroscopy, Corros. Sci. 52 (4) (2010) 1305–1316.

[18] Y.S. Chu, I.K. Robinson, A.A. Gewirth, Comparison of aqueous and native oxide formation on Cu(111), J. Chem. Phys. 110 (12) (1999) 5952–5959.

[19] S.K. Chawla, B.I. Rickett, N. Sankarraman, J.H. Payer, An X-ray photo-electron spectroscopic investigation of the air-formed film on copper, Corros. Sci. 33 (10) (1992) 1617–1631.

[20] I. Platzman, R. Brener, H. Haick, R. Tannenbaum, Oxidation of polycrystalline copper thin films at ambient conditions, J. Phys. Chem. C 112 (4) (2008) 1101–1108.

[21] J. Iijima, J.-W. Lim, S.-H. Hong, S. Suzuki, K. Mimura, M. Isshiki, Native oxidation of ultra high purity Cu bulk and thin films, Appl. Surf. Sci. 253 (5) (2006) 2825–2829.

[22] N. Cabrera, N.F. Mott, Theory of the oxidation of metals, Rep. Prog. Phys. 12 (1) (1949) 163–184.

[23] J.-W. Lim, Y. Ishikawa, K. Miyake, M. Yamashita, M. Isshiki, Influence of substrate bias voltage on the properties of Cu thin films by sputter type ion beam deposition, Mater. Trans. 43 (6) (2002) 1403–1408.

[24] J.W.M. Frenken, I.M.N. Groot, Operando Research in Heterogeneous Catalysis. Springer: Cham, Switzerland, 2017, Vol. 114.

[25] L. Luo, Y. Kang, J.C. Yang, G. Zhou, Effect of oxygen gas pressure on orientations of Cu2O nuclei during the initial oxidation of Cu(100), (110) and (111), Surf. Sci. 606 (23-24) (2012) 1790–1797.

[26] A. Posada-Borbon, B. Hagman, A. Schaefer, C. Zhang, M. Shipilin, A. Hellman, J. Gustafson, H. Gronbeck, Initial oxidation of Cu(100) studied by X-ray photo-electron spectroscopy and density functional theory calculations, Surf. Sci. 675 (2018) 64–69.

[27] J. Wang, C. Li, Y. Zhu, J.A. Boscoboinik, G. Zhou, Insight into the Phase Transformation Pathways of Copper Oxidation: From Oxygen Chemisorption on the Clean Surface to Multilayer Bulk Oxide Growth, J. Phys. Chem. C 122 (46) (2018) 26519–26527.

[28] D. Frank Ogletree, H. Bluhm, E.D. Hebenstreit, M. Salmeron, Photoelectron spectroscopy under ambient pressure and temperature conditions, Nucl. Instrum. Methods Phys. Res. Sect. A-Accelerat. Spectrom. Detect. Associat. Equipment 601 (1-2) (2009) 151–160.

[29] H. Bluhm, K. Andersson, T. Araki, K. Benzerara, G.E. Brown, J.J. Dynes, S. Ghosal, M.K. Gilles, H.-C. Hansen, J.C. Hemminger, A.P. Hitchcock, G. Ketteler, A.L.D. Kilcoyne, E. Kneedler, J.R. Lawrence, G.G. Leppard, J. Majzlam, B.S. Mun, S.C.B. Myneni, A. Nilsson, H. Ogasawara, D.F. Ogletree, K. Pecher, M. Salmeron, D.K. Shuh, B. Tonner, T. Tyliszczak, T. Warwick, T.H. Yoon, Soft X-ray microscopy and spectroscopy at the molecular environmental science beamline at the Advanced Light Source, J. Electron Spectrosc. Relat. Phenom. 150 (2-3) (2006) 86–104.

[30] M.O. Krause, J.H. Oliver, Natural widths of atomic k-levels and l-levels, k-alpha X-ray-lines and several kll Auger lines, J. Phys. Chem. Ref. Data 8 (2) (1979) 329–338.

[31] H. Tillborg, A. Nilsson, B. Hernnas, N. Martensson, O/CU(100) studied by core level spectroscopy, Surf. Sci. 269 (1992) 300–304.

[32] A.I. Stadnichenko, A.M. Sorokin, A.I. Boronin, XPS, UPS, and STM studies of nanostructured CuO films, J. Struct. Chem. 49 (2) (2008) 341–347.

[33] P. Jiang, D. Prendergast, F. Borondics, S. Porsgaard, L. Giovanetti, E. Pach, J. Newberg, H. Bluhm, F. Besenbacher, M. Salmeron, Experimental and theoretical investigation of the electronic structure of Cu2O and CuO thin films on Cu(110) using x-ray photoelectron and absorption spectroscopy, J. Chem. Phys. 138 (2) (2013) 024704, https://doi.org/10.1063/1.4773583.

[34] C.D. Wagner; A.V. Naumkin; J.W. Allison; C.J. Powell; Rumble, J. R. J. NIST Standard Reference Database 20, Version 3.4. http://srdata.nist.gov/xps/.

[35] S. Tanuma, C.J. Powell, D.R. Penn, Calculations of electron inelastic mean free paths.2. data for 27 elements over the 50–2000-eV range, Surf. Interface Anal. 17 (13) (1991) 911–926.

[36] M. Çopuroğlu, H. Sezen, R.L. Opila, S. Suzer, Band-bending at buried SiO2/Si interface as probed by XPS, ACS Appl. Mater. Interfaces 5 (12) (2013) 5875–5881.

[37] L.H. Dubois, Oxygen-chemisorption and cuprous-oxide formation on cu(111) - a high-resolution EELS study, Surf. Sci. 119 (2-3) (1982) 399–410.

[38] R.N. Lee, Farnswor He, Leed studies of adsorption on clean (100) copper surfaces, Surf. Sci., 1965, 3 (5), 461-&.

[39] T. Yokoyama, D. Arvanitis, T. Lederer, M. Tischer, L. Troger, K. Baberschke, G. Comelli, Adsorption of oxygen on cu(100).2. molecular adsorption and dissociation by means of o-k-edge X-ray-absorption fine-structure, Phys. Rev. B 48 (20) (1993) 15405–15416.

[40] T. Sueyoshi, T. Sasaki, Y. Iwasawa, Molecular and atomic adsorption states of oxygen on Cu(111) at 100–300 K, Surf. Sci. 365 (2) (1996) 310–318.

[41] G. Ketteler, D.F. Ogletree, H. Bluhm, H. Liu, E.L.D. Hebenstreit, M. Salmeron, In situ spectroscopic study of the oxidation and reduction of Pd(111), J. Am. Chem. Soc. 127 (51) (2005) 18269–18273.

[42] M. Lee, A.J.H. McGaughey, Role of sub-surface oxygen in Cu(100) oxidation, Surf. Sci. 604 (17-18) (2010) 1425–1431.

[43] T. Lederer, D. Arvanitis, G. Comelli, L. Tröger, K. Baberschke, Adsorption of oxygen on Cu (100). I. local structure and dynamics for two atomic chemisorption states, Phys. Rev. B 48 (20) (1993) 15390–15404.

[44] M. Harrison, D. Woodruff, J. Robinson, D. Sander, W. Pan, J. Kirschner, Adsorbate-induced surface reconstruction and surface-stress changes in Cu (100)/ O: Experiment and theory, Phys. Rev. B 74 (16) (2006), 165402.

[45] L. Trotochaud, A.R. Head, S. Pletincx, O. Karslıoğlu, Y.i. Yu, A. Waldner, L. Kyhl, T. Hauffman, H. Terryn, B. Eichhorn, H. Bluhm, Water Adsorption and Dissociation on Polycrystalline Copper Oxides: Effects of Environmental Contamination and Experimental Protocol, J. Phys. Chem. B 122 (2) (2018) 1000–1008.